

UDC 534.12:624.073.8]:519.6

Original scientific paper

Received: 22.03.2016.

Static and dynamic rectangular finite elements for plate vibration analysis

Ivo Senjanović, Marko Tomić, Neven Hadžić, Nikola Vladimir

University of Zagreb, Faculty of Mechanical Engineering and Naval Architecture, Zagreb, CROATIA

e-mail: ivo.senjanovic@fsb.hr

SUMMARY

Nowadays dynamic finite elements with frequency dependent unified stiffness matrix are considered in order to reduce finite element mesh density, and, consequently, system of algebraic equations in eigenvalue formulation. In this paper, an attempt to develop a 4-noded rectangular finite element for thin plate bending is presented. Since there is no simple general analytical solution of plate vibrations for arbitrary boundary conditions, dynamic shape functions are assumed as products of beam shape functions in longitudinal and transverse direction. Dynamic finite element with frequency dependent stiffness and mass matrix is derived by energy approach. Convergence of results is checked and it is found that such finite element formulation is not suitable for wider use. Therefore, strip finite element for vibration analysis of rectangular plate with simply supported two opposite edges is developed, which gives exact results. Application of both finite elements is illustrated by several numerical examples.

KEY WORDS: *thin plate, dynamic finite elements, rectangular element, strip element, dynamic stiffness and mass matrix.*

1. INTRODUCTION

The finite element method (FEM) is a numerical method in which physical properties from the element area are condensed into its nodes. In that way, the governing differential equations describing the behaviour of an element are transformed into the system of algebraic equations based on energy equivalence [1].

FEM is widely used for structural analysis of engineering structures due to the possibility of detailed modelling of complex structure topology and relatively easy computing. Depending on the type of structure, different finite elements have been developed for strength analysis, vibration analysis, stability analysis, etc. [1]. At the very beginning of computer application, matrix methods have been developed as a basis for later development of nowadays generally accepted FEM [2, 3]. Two FEM formulations have been developed, i.e. the displacement finite element method and force finite element method. In the former and latter case, nodal

displacements and nodal forces are unknown, respectively. Nowadays, the displacement FEM is mostly used as a more practical solution [1].

This paper deals with thin plate vibration analysis [4]. For this purpose, two types of 4-noded rectangular finite elements are used; one with deflection compatibility (non-conforming) and the other with deflection and slope compatibility (conforming) [2]. In both cases, shape functions are presented in polynomial form. Static stiffness and mass matrix are developed. Numerical solution converges to the exact one by increasing finite element mesh density.

Nowadays, there is a tendency to develop dynamic finite elements with dynamic stiffness. For this purpose, analytical solution of differential equation of motion is used. However, that is a relatively easy task if 1D problems as bars and beams are considered, or if 2D problem can be reduced to 1D problem, as in the case of plate with simply supported two opposite edges [5]. An advantage of dynamic finite elements is the applicability of coarser finite element mesh and high accuracy.

In this paper, an attempt to develop a dynamic 4-noded rectangular finite element with frequency dependent stiffness and mass matrix is described. Shape functions are assumed in the form of products of the analytical beam shape functions. Since such plate shape functions are an approximation of the real ones, the usual energy approach is applied. Also, dynamic strip finite element for vibration analysis of plates with simply supported two opposite edges is presented. Its application is illustrated in several numerical examples. Depending on boundary conditions, both displacement and force finite element methods are used in order to avoid the ill-conditioned formulation of eigenvalue problem and a rather complicated procedure for its solving [6].

2. STATE-OF-THE ART

2.1 GENERAL

There are two basic 4-noded rectangular plate bending finite elements. One satisfies only deflection compatibility conditions along the edges, and the other both deflection and slope compatibility conditions. The former is called a non-conforming element and may yield over or under-stiff results. The latter is called a conforming element and demonstrates monotonic convergence from the over-stiff side to the exact solution [1, 2].

Shape functions of the non-conforming element are expressed in polynomial terms based on static plate deformation. Shape functions of conforming element are defined as product of beam shape functions in longitudinal and transversal directions. The element properties, i.e. stiffness matrix, mass matrix, geometric stiffness matrix and load vector for static, dynamic and stability analyses, are based on the variation principle or energy approach, and are mainly presented in symbolic form.

2.2 FINITE ELEMENT WITH DEFLECTION COMPATIBILITY

The 4-noded rectangular finite element is shown in Figure 1 in Cartesian $(0, x, y)$ and natural $(0, \xi, \eta)$ coordinate systems.

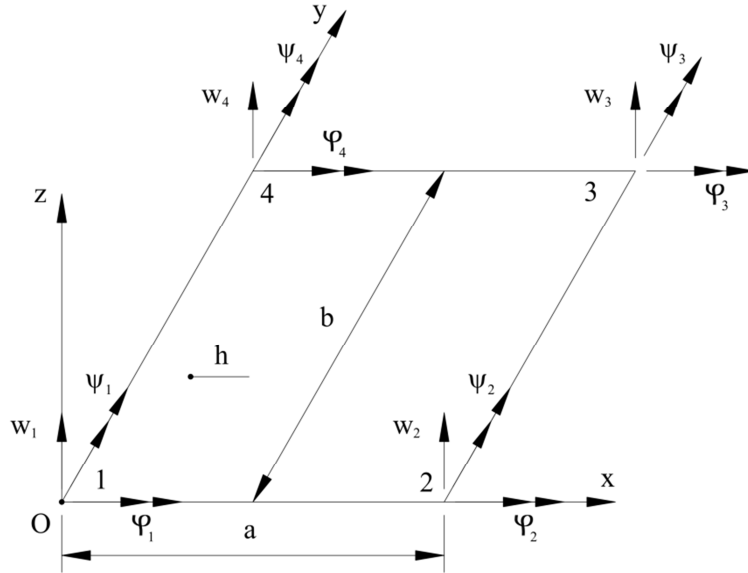


Fig. 1 Rectangular plate bending finite element with origin in node 1

Nodal displacements, i.e. nodal deflection and rotation angles are indicated. Deflection function is assumed in the polynomial form involving 12 terms equal to the number of degrees of freedom (DOF):

$$w = a_0 + a_1\xi + a_2\eta + a_3\xi^2 + a_4\xi\eta + a_5\eta^2 + a_6\xi^3 + a_7\xi^2\eta + a_8\xi\eta^2 + a_9\eta^3 + a_{10}\xi^3\eta + a_{11}\xi\eta^3, \quad (1)$$

where $\xi = x/a$, $\eta = y/b$ and a and b are finite element length and breadth, respectively. In Eq. (1) all polynomial terms of the third order and lower are included. Among 5 terms of the fourth order only two mixed terms i.e., $\xi^3\eta$ and $\xi\eta^3$ are taken into account as the best choice from the accuracy point of view.

Rotation angles are specified as:

$$\varphi = \frac{\partial w}{\partial y} = \frac{1}{b} \frac{\partial w}{\partial \eta}, \quad \psi = -\frac{\partial w}{\partial x} = -\frac{1}{a} \frac{\partial w}{\partial \xi}. \quad (2)$$

Shape functions, i.e. deflection functions due to unit value of one nodal displacement (deflection or rotation) and zero value of the others, are obtained in the following form:

$$\{\Phi\} = \left\{ \begin{array}{l} 1 - \xi\eta - (3 - 2\xi)\xi^2(1 - \eta) - (1 - \xi)(3 - 2\eta)\eta^2 \\ (1 - \xi)\eta(1 - \eta)^2 b \\ -\xi(1 - \xi)^2(1 - \eta)a \\ (3 - 2\xi)\xi^2(1 - \eta) + \xi\eta(1 - \eta)(1 - 2\eta) \\ \xi\eta(1 - \eta)^2 b \\ (1 - \xi)\xi^2(1 - \eta)a \\ (3 - 2\xi)\xi^2\eta - \xi\eta(1 - \eta)(1 - 2\eta) \\ -\xi(1 - \eta)\eta^2 b \\ (1 - \xi)\xi^2\eta a \\ (1 - \xi)(3 - 2\eta)\eta^2 + \xi(1 - \xi)(1 - 2\xi)\eta \\ -(1 - \xi)(1 - \eta)\eta^2 b \\ -\xi(1 - \xi)^2\eta a \end{array} \right\} \quad (3)$$

Shape functions due to unit nodal displacements w_i are of order $\xi^3\eta$ and $\xi\eta^3$, as well as those for unit nodal rotation angle φ and ψ , i.e. $\xi\eta^3$ and $\xi^3\eta$, respectively. The above shape functions and corresponding stiffness matrix in symbolic form are shown in Refs. [1, 7]. Moreover, stiffness and mass matrix in symbolic form are presented in Refs. [4, 8, 9].

2.3 FINITE ELEMENT WITH DEFLECTION AND SLOPE COMPATIBILITY

Finite element shown in Figure 1 is considered. Shape functions $\Phi_j(\xi, \eta)$, $j = 1, 2, \dots, 12$, are specified as products of beam shape functions in ξ and η directions, $X_i(\xi)$ and $Y_i(\eta)$, $i = 1, 2, 3, 4$ [2]:

$$\begin{aligned} \Phi_1 &= X_1 Y_1 = (1 + 2\xi)(1 - \xi)^2(1 + 2\eta)(1 - \eta)^2 \\ \Phi_2 &= X_1 Y_2 = (1 + 2\xi)(1 - \xi)^2\eta(1 - \eta)^2 b \\ \Phi_3 &= -X_2 Y_1 = -\xi(1 - \xi)^2(1 + 2\eta)(1 - \eta)^2 a \\ \Phi_4 &= X_3 Y_1 = (3 - 2\xi)\xi^2(1 + 2\eta)(1 - \eta)^2 \\ \Phi_5 &= X_3 Y_2 = (3 - 2\xi)\xi^2\eta(1 - \eta)^2 b \\ \Phi_6 &= -X_4 Y_1 = (1 - \xi)\xi^2(1 + 2\eta)(1 - \eta)^2 a \\ \Phi_7 &= X_3 Y_3 = (3 - 2\xi)\xi^2(3 - 2\eta)\eta^2 \\ \Phi_8 &= X_3 Y_4 = -(3 - 2\xi)\xi^2(1 - \eta)\eta^2 b \\ \Phi_9 &= -X_4 Y_3 = (1 - \xi)\xi^2(3 - 2\eta)\eta^2 a \\ \Phi_{10} &= X_1 Y_3 = (1 + 2\xi)(1 - \xi^2)(3 - 2\eta)\eta^2 \\ \Phi_{11} &= X_1 Y_4 = -(1 + 2\xi)(1 - \xi)^2(1 - \eta)\eta^2 b \\ \Phi_{12} &= -X_2 Y_3 = -\xi(1 - \xi)^2(3 - 2\eta)\eta^2 a. \end{aligned} \quad (4)$$

In this case, all shape functions are of $\xi^3\eta^3$ order. Stiffness matrix is shown in the symbolic form in Ref. [2], while both stiffness and mass matrices are specified in Ref. [9].

3. FINITE ELEMENT BASED ON FREE PLATE NATURAL MODES

Finite element of a vibrating plate can be considered as a free structural element in space. Therefore, it is reasonable to assume its deflection function as a set of free plate natural modes. Only natural vibrations of plates with simply supported two opposite edges and arbitrary boundary conditions on the remaining two edges can be determined analytically in a relatively simple way. Strictly speaking, some other boundary value problems are also solved analytically but in a very complicated manner [10, 11]. Therefore, for arbitrary boundary conditions, numerical methods like Rayleigh-Ritz method, finite difference method and finite element method (FEM) are preferred. However, natural vibrations of a free plate can also be analysed approximately in a simple analytical way by the Rayleigh quotient, if the mode shapes are assumed in the form of products of free beam natural modes, $W(\xi, \eta) = X(\xi)Y(\eta)$ [12].

Beam natural modes are divided into two groups, i.e. symmetric and antisymmetric. Therefore, the origin of the coordinate system is located in the middle of the beam length, $l = 2a$. Free beam natural modes are expressed by the natural coordinate $\xi = x/a$, as follows [12]:

symmetric:

$$X_0 = 1, \quad X_i = \frac{1}{2} \left(\frac{\cosh \gamma_i \xi}{\cosh \gamma_i} + \frac{\cos \gamma_i \xi}{\cos \gamma_i} \right), \quad i = 2, 4, \dots \quad \gamma_2 = 2.3650, \quad \gamma_4 = 5.4978, \dots \quad (5)$$

antisymmetric:

$$X_1 = \xi, \quad X_i = \frac{1}{2} \left(\frac{\sinh \gamma_i \xi}{\sinh \gamma_i} + \frac{\sin \gamma_i \xi}{\sin \gamma_i} \right), \quad i = 3, 5, \dots \quad \gamma_3 = 3.9266, \quad \gamma_5 = 7.0686, \dots \quad (6)$$

The same expressions are valid for beam natural modes in the cross-direction $\eta = y/b$, denoted as $Y_i(\eta)$.

The first three plate natural modes are due to rigid body motion with zero natural frequencies since there is no restoring stiffness. Finite element vibration analysis of a free square plate shows that elastic natural modes are of ordinary form [12]:

$$W_{ij}(\xi, \eta) = X_i(\xi)Y_j(\eta), \quad (7)$$

or extraordinary form:

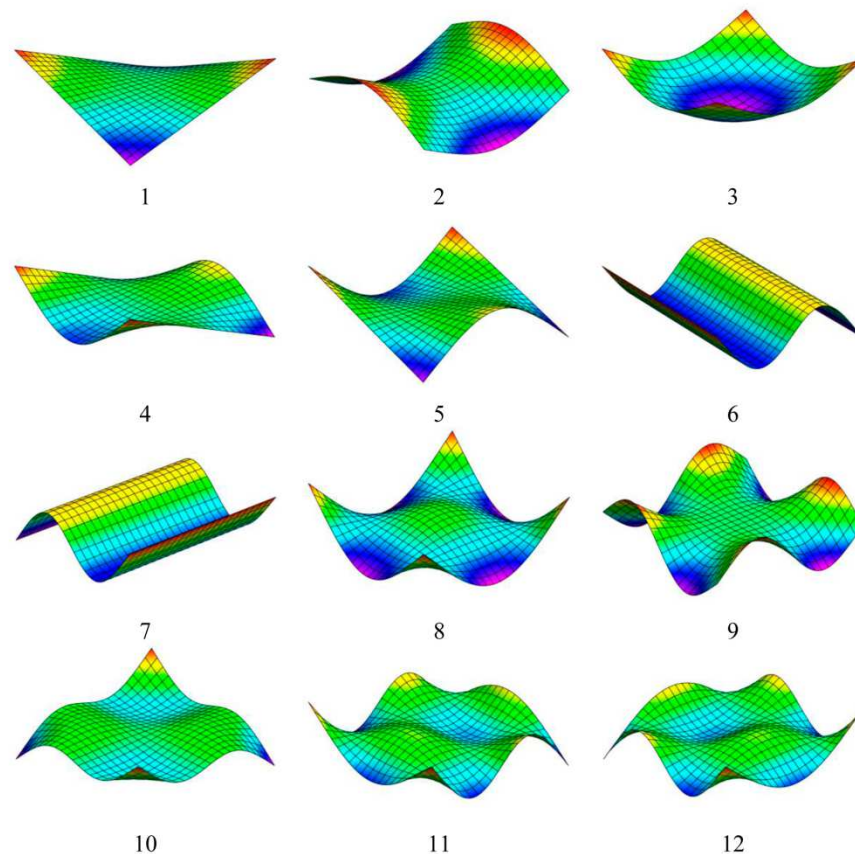
$$W_{mn \pm kl}(\xi, \eta) = X_m(\xi)Y_n(\eta) \pm X_k(\xi)Y_l(\eta). \quad (8)$$

The first 12 elastic natural modes are shown in Figure 2 and the corresponding formulae are specified in Table 1. Shapes of the 2nd and 3rd modes are a hyperbolic and an elliptical paraboloid, respectively [12]. Dimensionless frequency parameters determined by both FEM analysis and the Rayleigh quotient (RQ) are listed in Table 1. Their accuracy is estimated with respect to the reliable results determined by the Rayleigh-Ritz method (RRM) in Ref. [13].

Table 1 Frequency parameter $\Omega = \omega(2b/\pi)^2 \sqrt{\rho h/D}$ of free square plate elastic modes, Figure 3

Mode no.	Mode type	FEM	Discrepancy %	RQ	Discrepancy %	RRM, Liew [13]
1	X_1Y_1	1.3631	-0.11	1.4386	5.42	1.3646
2	$X_2Y_0 - X_0Y_2$	1.9827	-0.15	2.0186	1.66	1.9856
3	$X_2Y_0 + X_0Y_2$	2.4564	-0.11	2.4906	1.28	2.4590
4	X_1Y_2	3.5185	-0.21	3.6977	4.87	3.5260
5	X_2Y_1	3.5185	-0.21	3.6977	4.87	3.5260
6	$X_3Y_0 - X_0Y_3$	6.1772	-0.21	6.2488	0.95	6.1900
7	$X_3Y_0 + X_0Y_3$	6.1772	-0.21	6.2488	0.95	6.1900
8	X_2Y_2	6.4317	-0.32	6.8116	5.56	6.4526
9	$X_3Y_1 - X_1Y_3$	6.9930	-0.35	7.0710	0.76	7.0179
10	$X_3Y_1 + X_1Y_3$	7.7798	-0.50	8.1036	3.64	7.8190
11	X_2Y_3	10.6340		11.1865	(5.20)*	
12	X_3Y_2	10.6340		11.1865	(5.20)*	

* With respect to FEM

**Fig. 2** Free square plate natural modes, FEM

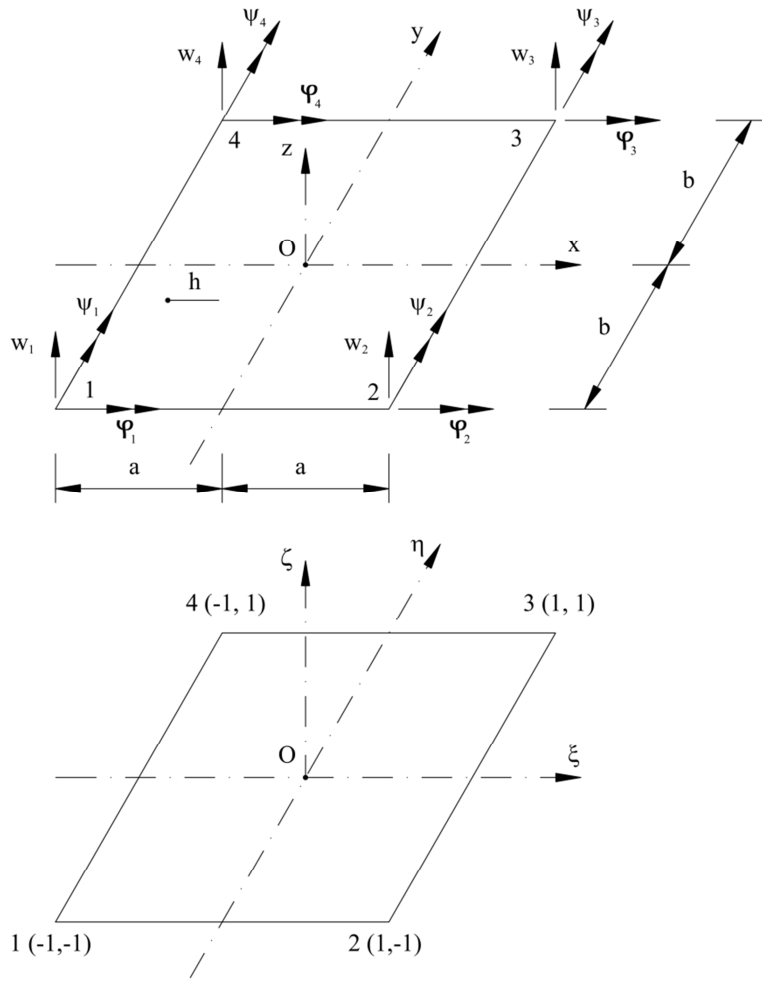


Fig. 3 Rectangular plate bending finite element in Cartesian and natural coordinate systems

It is necessary to point out that extraordinary modes for rectangular plate move to higher frequencies by increasing value of the plate aspect ratio a/b . Therefore, deflection of rectangular finite element shown in Figure 3 is assumed as a set of three rigid body modes and 9 square plate elastic modes. Ordinary modes and constitutive parts of extraordinary modes are taken into account. Symmetric mode X_2Y_2 is excluded. Hence, one can write:

$$W(\xi, \eta) = \langle P(\xi, \eta) \rangle \{a\}, \quad (9)$$

where $\{a\}$ is vector of unknown coefficients and:

$$\langle P(\xi, \eta) \rangle = \langle 1 \ \xi \ \eta \ \xi\eta \ X_2 \ Y_2 \ X_3 \ X_2\eta \ \xi Y_2 \ Y_3 \ X_3\eta \ \xi Y_3 \rangle. \quad (10)$$

Structure of $\langle P(\xi, \eta) \rangle$ is similar to the polynomial terms in the case of finite element with deflection compatibility conditions, Eq. (1).

For rotation angles, the following is obtained:

$$\begin{aligned} \varphi &= \frac{1}{b} \frac{\partial w}{\partial \eta} = \frac{1}{b} \frac{\partial \langle P \rangle}{\partial \eta} \{a\} \\ \psi &= -\frac{1}{a} \frac{\partial w}{\partial \xi} = -\frac{1}{a} \frac{\partial \langle P \rangle}{\partial \xi} \{a\}, \end{aligned} \quad (11)$$

where:

$$\begin{aligned}\frac{\partial \langle P \rangle}{\partial \eta} &= \langle 0 \ 0 \ 1 \ \xi \ 0 \ Y'_2 \ 0 \ X_2 \ \xi Y'_2 \ Y'_3 \ X_3 \ \xi Y'_3 \rangle \\ \frac{\partial \langle P \rangle}{\partial \xi} &= \langle 0 \ 1 \ 0 \ \eta \ X'_2 \ 0 \ X'_3 \ X'_2 \eta \ Y'_2 \ 0 \ X'_3 \eta \ Y'_3 \rangle.\end{aligned}\quad (12)$$

Displacement field is specified as:

$$\{f\} = \begin{Bmatrix} w \\ \varphi \\ \psi \end{Bmatrix} = [Z(\xi, \eta)] \{a\}, \quad (13)$$

where:

$$[Z(\xi, \eta)] = \begin{bmatrix} \langle P \rangle \\ \frac{1}{b} \frac{\partial \langle P \rangle}{\partial \eta} \\ -\frac{1}{a} \frac{\partial \langle P \rangle}{\partial \xi} \end{bmatrix}. \quad (14)$$

Displacement vector of the i -th node according to Eq. (13) reads:

$$\{\delta\}_i = \begin{Bmatrix} w_i \\ \varphi_i \\ \psi_i \end{Bmatrix} = [Z]_i \{a\}, \quad i = 1, 2, 3, 4 \quad (15)$$

and the finite element displacement vector:

$$\{\delta\} = \{\{\delta\}_i\} = [Z] \{a\}, \quad (16)$$

where:

$$[Z] = \begin{bmatrix} [Z]_1 \\ [Z]_2 \\ [Z]_3 \\ [Z]_4 \end{bmatrix}. \quad (17)$$

By substituting $\{a\}$ from Eq. (16) into Eq. (9) one can express deflection function by the nodal displacement vector:

$$w(\xi, \eta) = \langle \Phi \rangle \{\delta\}, \quad (18)$$

where:

$$\langle \Phi \rangle = \langle P(\xi, \eta) \rangle [Z]^{-1} \quad (19)$$

is vector of shape functions.

Deformation (curvature) vector is obtained in the form:

$$\{\kappa\} = - \begin{Bmatrix} \frac{\partial^2 w}{\partial x^2} \\ \frac{\partial^2 w}{\partial y^2} \\ 2 \frac{\partial^2 w}{\partial x \partial y} \end{Bmatrix} = [B] \{\delta\}, \quad (20)$$

where:

$$[B] = -[A][Z]^{-1} \quad (21)$$

$$[A] = \begin{Bmatrix} \frac{1}{a^2} \left\langle \frac{\partial^2 P}{\partial \xi^2} \right\rangle \\ \frac{1}{b^2} \left\langle \frac{\partial^2 P}{\partial \eta^2} \right\rangle \\ \frac{2}{ab} \left\langle \frac{\partial^2 P}{\partial \xi \partial \eta} \right\rangle \end{Bmatrix} = \begin{Bmatrix} \frac{1}{a^2} \langle p \rangle \\ \frac{1}{b^2} \langle q \rangle \\ \frac{2}{ab} \langle r \rangle \end{Bmatrix} \quad (22)$$

$$\begin{aligned} \langle p \rangle &= \langle 0 \quad 0 \quad 0 \quad 0 \quad X_2'' \quad 0 \quad X_3'' \quad X_2'' \eta \quad 0 \quad 0 \quad X_3'' \eta \quad 0 \rangle \\ \langle q \rangle &= \langle 0 \quad 0 \quad 0 \quad 0 \quad 0 \quad Y_2'' \quad 0 \quad 0 \quad \xi Y_2'' \quad Y_3'' \quad 0 \quad \xi Y_3'' \rangle \\ \langle r \rangle &= \langle 0 \quad 0 \quad 0 \quad 1 \quad 0 \quad 0 \quad 0 \quad X_2' \quad Y_2' \quad 0 \quad X_3' \quad Y_3' \rangle. \end{aligned} \quad (23)$$

According to the definition of stiffness matrix [1]:

$$[K] = \int_A [B]^T [D] [B] dA, \quad (24)$$

where:

$$[D] = D[d], \quad D = \frac{Eh^3}{12(1-\nu^2)}, \quad [d] = \begin{Bmatrix} 1 & \nu & 0 \\ \nu & 1 & 0 \\ 0 & 0 & \frac{1-\nu}{2} \end{Bmatrix} \quad (25)$$

is a matrix of flexural rigidity, the following is obtained by employing Eq. (21):

$$[K] = Dab \left([Z]^{-1} \right)^T [k] [Z]^{-1}, \quad (26)$$

where:

$$[k] = \int_{-1}^1 \int_{-1}^1 [A]^T [d] [A] d\xi d\eta. \quad (27)$$

Taking into account Eq. (22), the element of matrix $[k]$ can be written in index notation:

$$k_{ij} = \frac{1}{a^2 b^2} \int_{-1}^1 \int_{-1}^1 \left\{ p_i \left[\left(\frac{b}{a} \right)^2 p_j + \nu q_j \right] + q_i \left[\left(\frac{a}{b} \right)^2 q_j + \nu p_j \right] + 2(1-\nu) r_i r_j \right\}, \quad (28)$$

where p_i , q_i and r_i are defined by Eq. (23).

Mass matrix is expressed with shape functions:

$$[M] = \bar{m} \int_A \{\Phi\} \langle \Phi \rangle dA, \quad (29)$$

where $\bar{m} = \rho h$ is mass per unit plate area. By substituting Eq. (19) into Eq. (29), the following is obtained:

$$[M] = \bar{m} a b \left([Z]^{-1} \right)^T [J] [Z]^{-1}, \quad (30)$$

where:

$$[J] = \int_{-1}^1 \int_{-1}^1 \{P\} \langle P \rangle d\xi d\eta. \quad (31)$$

The finite element equation reads:

$$\{F\} = ([K] - \omega^2 [M]) \{\delta\}, \quad (32)$$

where $\{F\}$ and $\{\delta\}$ are vectors of nodal forces and nodal displacements, respectively.

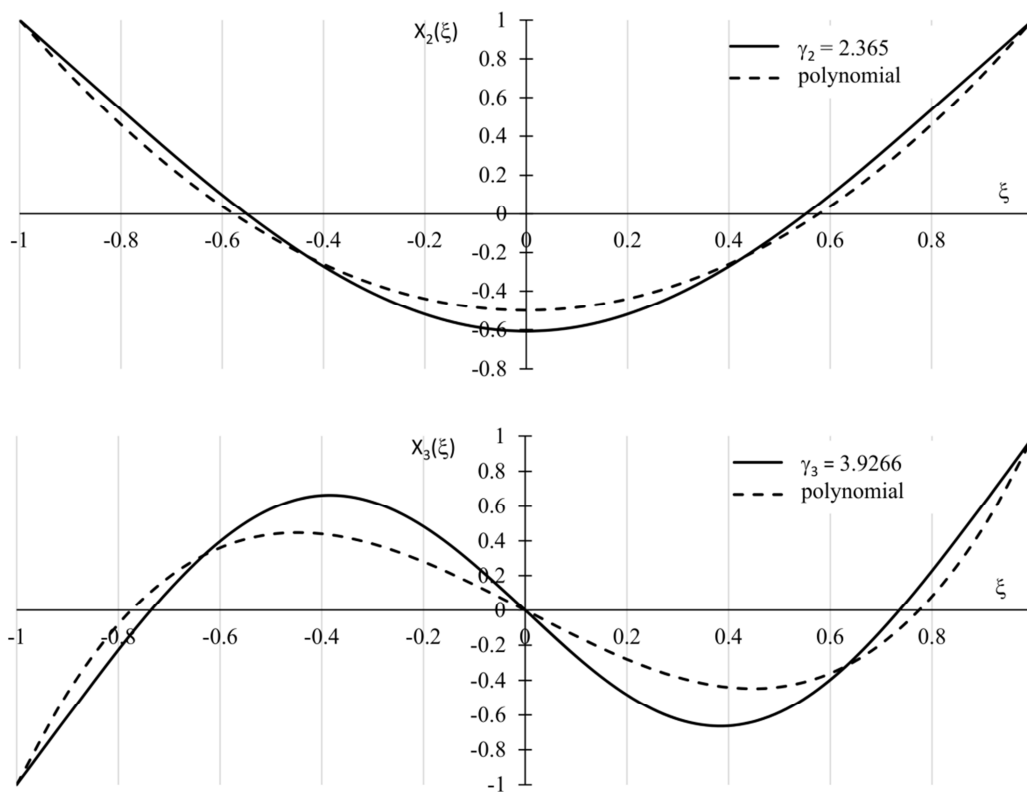
The first two free beam natural modes, Eqs. (5) and (6), are shown in Figure 4. Vibration analysis of free square plate modelled by the presented finite element shows that all 12 natural frequencies determined by only one finite element agree very well with the exact solution, whereas for dense finite element mesh results converge to slightly higher values of the exact ones, Table 2. Therefore, beam natural modes, Eqs. (5) and (6), are approximated by polynomials:

$$X_2 = \frac{1}{2} (3\xi^2 - 1), \quad X_3 = \frac{1}{2} \xi (5\xi^2 - 3) \quad (33)$$

and compared in Figure 4. Discrepancies of natural frequencies of free square plate determined by one finite element are very large for higher modes. However, the results rapidly converge to the exact solution by increasing the finite element mesh density, Table 2.

Table 2 Frequency parameter $\Omega = \omega(2b/\pi)^2 \sqrt{\rho h/D}$ of free square plate, Figure 3

Mode No.	Liew [13]	Free plate		Polynomial, mesh				
		modes, mesh 1x1	1x1	2x2	4x4	6x6	8x8	10x10
1	1.3646	1.3081	1.3873	1.3807	1.3699	1.3674	1.3662	1.3654
2	1.9856	2.0190	2.2710	1.9819	1.9922	1.9889	1.9874	1.9866
3	2.4590	2.3646	3.1008	2.4436	2.4741	2.4666	2.4634	2.4618
4	3.5260	3.3074	4.1221	3.4155	3.5156	3.5231	3.5249	3.5254
5	3.5260	3.3074	4.1221	3.4155	3.5156	3.5231	3.5249	3.5254
6	6.1900	5.9934	9.1783	6.4280	6.2594	6.2295	6.2136	6.2054
7	6.1900	5.9934	9.4354	7.0565	6.2594	6.2295	6.2136	6.2054
8	6.4526	6.1829	9.4354	7.0565	6.3479	6.3943	6.4184	6.4305
9	7.0179	7.0672	10.5612	7.6572	7.0537	7.0462	7.0369	7.0311
10	7.8190			8.9303	7.6266	7.7497	7.7835	7.7976

**Fig. 4** The first two free beam elastic modes and their polynomial approximation

Based on the aforesaid numerical test, the polynomially approximated beam natural modes, Eq. (33), are used for the derivation of finite element properties. That also enables their symbolical presentation.

Matrix of the polynomial coefficients and its inversion read:

$$[Z] = \begin{bmatrix} \langle 1 & -1 & -1 & 1 & 1 & 1 & -1 & -1 & -1 & -1 & 1 & 1 \rangle \\ \frac{1}{b} \langle 0 & 0 & 1 & -1 & 0 & -3 & 0 & 1 & 3 & 6 & -1 & -6 \rangle \\ \frac{1}{a} \langle 0 & -1 & 0 & 1 & 3 & 0 & -6 & -3 & -1 & 0 & 6 & 1 \rangle \\ \langle 1 & 1 & -1 & -1 & 1 & 1 & 1 & -1 & 1 & -1 & -1 & -1 \rangle \\ \frac{1}{b} \langle 0 & 0 & 1 & 1 & 0 & -3 & 0 & 1 & -3 & 6 & 1 & 6 \rangle \\ \frac{1}{a} \langle 0 & -1 & 0 & 1 & -3 & 0 & -6 & 3 & -1 & 0 & 6 & 1 \rangle \\ \langle 1 & 1 & 1 & 1 & 1 & 1 & 1 & 1 & 1 & 1 & 1 & 1 \rangle \\ \frac{1}{b} \langle 0 & 0 & 1 & 1 & 0 & 3 & 0 & 1 & 3 & 6 & 1 & 6 \rangle \\ \frac{1}{a} \langle 0 & -1 & 0 & -1 & -3 & 0 & -6 & -3 & -1 & 0 & -6 & -1 \rangle \\ \langle 1 & -1 & 1 & -1 & 1 & 1 & -1 & 1 & -1 & 1 & -1 & -1 \rangle \\ \frac{1}{b} \langle 0 & 0 & 1 & -1 & 0 & 3 & 0 & 1 & -3 & 6 & -1 & -6 \rangle \\ \frac{1}{a} \langle 0 & -1 & 0 & -1 & 3 & 0 & -6 & 3 & -1 & 0 & -6 & -1 \rangle \end{bmatrix} \quad (34)$$

$$[Z]^{-1} = \frac{1}{20} \begin{bmatrix} 5 & \frac{5}{3}b & -\frac{5}{3}a & 5 & \frac{5}{3}b & \frac{5}{3}a & 5 & -\frac{5}{3}b & \frac{5}{3}a & 5 & -\frac{5}{3}b & -\frac{5}{3}a \\ -6 & -\frac{5}{3}b & a & 6 & \frac{5}{3}b & a & 6 & -\frac{5}{3}b & a & -6 & \frac{5}{3}b & a \\ -6 & -b & \frac{5}{3}a & -6 & -b & -\frac{5}{3}a & 6 & -b & \frac{5}{3}a & 6 & -b & -\frac{5}{3}a \\ 7 & b & -a & -7 & -b & -a & 7 & -b & a & -7 & b & a \\ 0 & 0 & \frac{5}{3}a & 0 & 0 & -\frac{5}{3}a & 0 & 0 & -\frac{5}{3}a & 0 & 0 & \frac{5}{3}a \\ 0 & -\frac{5}{3}b & 0 & 0 & -\frac{5}{3}b & 0 & 0 & \frac{5}{3}b & 0 & 0 & \frac{5}{3}b & 0 \\ 1 & 0 & -a & -1 & 0 & -a & -1 & 0 & -a & 1 & 0 & -a \\ 0 & 0 & -\frac{5}{3}a & 0 & 0 & \frac{5}{3}a & 0 & 0 & -\frac{5}{3}a & 0 & 0 & \frac{5}{3}a \\ 0 & \frac{5}{3}b & 0 & 0 & -\frac{5}{3}b & 0 & 0 & \frac{5}{3}b & 0 & 0 & -\frac{5}{3}b & 0 \\ 1 & b & 0 & 1 & b & 0 & -1 & b & 0 & -1 & b & 0 \\ -1 & 0 & a & 1 & 0 & a & -1 & 0 & -a & 1 & 0 & -a \\ -1 & -b & 0 & 1 & b & 0 & -1 & b & 0 & 1 & -b & 0 \end{bmatrix} \quad (35)$$

Shape functions, by using Eq. (19), can be presented in index notation for each node $i = 1, 2, 3, 4$:

$$\begin{aligned} \Phi_{i1} &= \frac{1}{8} \left[2 + \xi_i \xi (3 - \xi^2) + \eta_i \eta (3 - \eta^2) + \xi_i \eta_i \xi \eta (4 - \xi^2 - \eta^2) \right] \\ \Phi_{i2} &= \frac{1}{8} (1 + \xi_i \xi + \eta_i \eta + \xi_i \eta_i \xi \eta) (\eta^2 - 1) b \\ \Phi_{i3} &= \frac{1}{8} (1 + \xi_i \xi + \eta_i \eta + \xi_i \eta_i \xi \eta) (1 - \xi^2) a. \end{aligned} \quad (36)$$

Shape functions of the finite element are numbered as follows:

$$\Phi_k = \Phi_{ij}, \quad i = 1, 2, 3, 4, \quad j = 1, 2, 3, \quad (37)$$

where $k = 1, 2 \dots 12$.

Stiffness matrix $[K]$ is determined according to Eqs. (26), (27) and (28), and mass matrix $[M]$ according to Eqs. (30) and (31). Matrix $[J]$ in $[M]$ is diagonal since polynomial terms in Eq. (10), where $X_2(\xi)$ and $X_3(\xi)$ are specified by Eq. (33), and $Y_2(\eta)$ and $Y_3(\eta)$ in an analogous way, are orthogonal, i.e.

$$\text{diagonal } [J] = 4 \begin{pmatrix} 1 & \frac{1}{3} & \frac{1}{3} & \frac{1}{9} & \frac{1}{5} & \frac{1}{5} & \frac{1}{7} & \frac{1}{15} & \frac{1}{15} & \frac{1}{7} & \frac{1}{21} & \frac{1}{21} \end{pmatrix}. \quad (38)$$

Stiffness and mass matrix can be derived in a symbolic form. They are the same as those presented in Refs. [4, 9], since polynomial Eq. (10) with functions Eq. (33) can be rearranged into the form Eq. (1). The advantage of the present approach is the physical explanation of the polynomial terms as approximate free plate natural modes. As a result, polynomial terms $\xi^3\eta$ and $\xi\eta^3$ are chosen instead of ξ^4 and η^4 due to lower natural frequencies, i.e. strain energy, Table 1. Another advantage of the present formulation is the specification of the shape functions in index notation, which facilitates the programming of the finite element.

4. FINITE ELEMENT BASED ON BEAM NATURAL MODES

Finite element with the origin of the coordinate system placed in node 1 is considered, Figure 1. Its shape functions can be specified as the product of beam shape functions $X_i(\xi)$ and $Y_i(\eta)$, $i = 1, 2, 3, 4$, as follows:

$$\begin{array}{cccc} \text{Node1} & \text{Node2} & \text{Node3} & \text{Node4} \\ \Phi_1 = X_1Y_1 & \Phi_4 = X_3Y_1 & \Phi_7 = X_3Y_3 & \Phi_{10} = X_1Y_3 \\ \Phi_2 = X_1Y_2 & \Phi_5 = X_3Y_2 & \Phi_8 = X_3Y_4 & \Phi_{11} = X_1Y_4 \\ \Phi_3 = -X_2Y_1 & \Phi_6 = -X_4Y_1 & \Phi_9 = -X_4Y_3 & \Phi_{12} = -X_2Y_3 \end{array}. \quad (39)$$

Plate deflection is presented in the form:

$$w(\xi, \eta) = \langle \Phi \rangle \{ \delta \}, \quad (40)$$

where $\langle \Phi \rangle$ is the vector of shape functions and $\{ \delta \}$ is the vector of nodal displacements.

Curvature vector is defined as:

$$\{ \kappa \} = - \begin{Bmatrix} \frac{\partial^2 w}{\partial x^2} \\ \frac{\partial^2 w}{\partial y^2} \\ 2 \frac{\partial^2 w}{\partial x \partial y} \end{Bmatrix} = - [B] \{ \delta \}, \quad (41)$$

where:

$$[B] = \begin{Bmatrix} \frac{1}{a^2} \left\langle \frac{\partial^2 \Phi}{\partial \xi^2} \right\rangle \\ \frac{1}{b^2} \left\langle \frac{\partial^2 \Phi}{\partial \eta^2} \right\rangle \\ \frac{2}{ab} \left\langle \frac{\partial^2 \Phi}{\partial \xi \partial \eta} \right\rangle \end{Bmatrix} = \begin{Bmatrix} \frac{1}{a^2} \langle p \rangle \\ \frac{1}{b^2} \langle q \rangle \\ \frac{2}{ab} \langle r \rangle \end{Bmatrix} \quad (42)$$

$$\begin{aligned}
\langle p \rangle &= \langle X_1'' Y_1 \quad X_1'' Y_2 \quad -X_2'' Y_1 \quad X_3'' Y_1 \quad X_3'' Y_2 \quad -X_4'' Y_1 \quad X_3'' Y_3 \quad X_3'' Y_4 \quad -X_4'' Y_3 \quad X_1'' Y_3 \quad X_1'' Y_4 \quad -X_2'' Y_3 \rangle \\
\langle q \rangle &= \langle X_1' Y_1'' \quad X_1' Y_2'' \quad -X_2' Y_1'' \quad X_3' Y_1'' \quad X_3' Y_2'' \quad -X_4' Y_1'' \quad X_3' Y_3'' \quad X_3' Y_4'' \quad -X_4' Y_3'' \quad X_1' Y_3'' \quad X_1' Y_4'' \quad -X_2' Y_3'' \rangle \\
\langle r \rangle &= \langle X_1' Y_1' \quad X_1' Y_2' \quad -X_2' Y_1' \quad X_3' Y_1' \quad X_3' Y_2' \quad -X_4' Y_1' \quad X_3' Y_3' \quad X_3' Y_4' \quad -X_4' Y_3' \quad X_1' Y_3' \quad X_1' Y_4' \quad -X_2' Y_3' \rangle.
\end{aligned} \quad (43)$$

Stiffness matrix is defined according to Eq. (24):

$$[K] = ab \int_0^1 \int_0^1 [B]^T [D] [B] d\xi d\eta = Dab[k], \quad (44)$$

where referring to Eq. (28):

$$k_{ij} = \frac{1}{a^2 b^2} \int_0^1 \int_0^1 \left[\left(\frac{b}{a} \right)^2 p_i p_j + \left(\frac{a}{b} \right)^2 q_i q_j + \nu (p_i q_j + q_i p_j) + 2(1-\nu) r_i r_j \right] d\xi d\eta. \quad (45)$$

Parameters p_i , q_i and r_i are specified by Eq. (43).

For mass matrix Eq. (29), one can write:

$$[M] = \bar{m}ab \int_0^1 \int_0^1 \{ \Phi \} \{ \Phi \} d\xi d\eta, \quad (46)$$

In order to determine beam shape functions, the deflection of a naturally vibrating beam with length l and natural coordinate $\xi = x/l$, $0 \leq \xi \leq 1$, is expressed by Krylov functions $U_i(\xi)$ due to simplicity:

$$X = A_1 U_1 + A_2 U_2 + A_3 U_3 + A_4 U_4, \quad (47)$$

where:

$$\begin{aligned}
U_1 &= \frac{1}{2}(ch\gamma\xi + \cos\gamma\xi) \\
U_2 &= \frac{1}{2}(sh\gamma\xi + \sin\gamma\xi) \\
U_3 &= \frac{1}{2}(ch\gamma\xi - \cos\gamma\xi) \\
U_4 &= \frac{1}{2}(sh\gamma\xi - \sin\gamma\xi).
\end{aligned} \quad (48)$$

An advantage of Krylov functions is their characteristic values at $\xi = 0$:

$$U_1(0) = 1, \quad U_2(0) = U_3(0) = U_4(0) = 0 \quad (49)$$

and relation between derivatives and functions:

$$\begin{aligned}
U_1' &= \gamma U_4, \quad U_2' = \gamma U_1, \quad U_3' = \gamma U_2, \quad U_4' = \gamma U_3 \\
U_1'' &= \gamma^2 U_3, \quad U_2'' = \gamma^2 U_4, \quad U_3'' = \gamma^2 U_1, \quad U_4'' = \gamma^2 U_2, \text{etc.}
\end{aligned} \quad (50)$$

Hence, derivatives of Krylov functions can be expressed by the same functions with the change of indexes in the anticlockwise direction.

Furthermore, one obtains for the angle of rotation:

$$\varphi = \frac{dX}{dx} = \frac{\gamma}{a} (A_1 U_4 + A_2 U_1 + A_3 U_2 + A_4 U_3). \quad (51)$$

The integration constants A_i can be expressed in terms of nodal displacements. For the 1st node $\xi=0$ and one finds from Eqs. (47) and (50) $A_1 = X(0) = W_1$, and $A_2 = \frac{a}{\gamma} \varphi(0) = \frac{a}{\gamma} \varphi_1$.

Constants A_3 and A_4 are expressed by A_1 and A_2 from the same equations setting for the 2nd node $X(1) = W_2$ and $\varphi(1) = \varphi_2$. Hence, deflection function Eq. (47) can be written in the form:

$$X(\xi) = X_1(\xi)W_1 + X_2(\xi)\varphi_1 + X_3(\xi)W_2 + X_4(\xi)\varphi_2, \quad (52)$$

where $X_i(\xi)$ refers to shape functions with unit value of deflection and rotation angle at $\xi=0$ and $\xi=1$, respectively:

$$\begin{aligned} X_1(\xi) &= U_1(\xi) + a_1 U_3(\xi) + b_1 U_4(\xi) \\ X_2(\xi) &= [U_2(\xi) + a_2 U_3(\xi) + b_2 U_4(\xi)] \frac{a}{\gamma} \\ X_3(\xi) &= a_3 U_3(\xi) + b_3 U_4(\xi) \\ X_4(\xi) &= [a_4 U_3(\xi) + b_4 U_4(\xi)] \frac{a}{\gamma} \end{aligned} \quad (53)$$

with the following coefficients:

$$\begin{aligned} a_1 &= \frac{1}{C} [U_1(1)U_3(1) - U_4^2(1)] = -\frac{sh\gamma \sin\gamma}{1 - ch\gamma \cos\gamma}, \\ a_2 &= -\frac{1}{C} [U_1(1)U_4(1) - U_2(1)U_3(1)] = -\frac{ch\gamma \sin\gamma - sh\gamma \cos\gamma}{1 - ch\gamma \cos\gamma}, \\ a_3 &= -\frac{1}{C} U_3(1) = \frac{ch\gamma - \cos\gamma}{1 - ch\gamma \cos\gamma}, \quad a_4 = \frac{1}{C} U_4(1) = -\frac{sh\gamma - \sin\gamma}{1 - ch\gamma \cos\gamma}, \\ b_1 &= \frac{1}{C} [U_3(1)U_4(1) - U_1(1)U_2(1)] = \frac{sh\gamma \cos\gamma + ch\gamma \sin\gamma}{1 - ch\gamma \cos\gamma}, \\ b_2 &= \frac{1}{C} [U_1(1)U_3(1) - U_2^2(1)] = \frac{sh\gamma \sin\gamma}{1 - ch\gamma \cos\gamma}, \\ b_3 &= \frac{1}{C} U_2(1) = -\frac{sh\gamma + \sin\gamma}{1 - ch\gamma \cos\gamma}, \quad b_4 = -\frac{1}{C} U_3(1) = \frac{ch\gamma - \cos\gamma}{1 - ch\gamma \cos\gamma}, \\ C &= U_2(1)U_4(1) - U_3^2(1) = -\frac{1}{2}(1 - ch\gamma \cos\gamma). \end{aligned} \quad (54)$$

The characteristic feature of the first shape function is that shear force:

$$Q(\xi) = -D \frac{d^3 X}{d\xi^3} = -\frac{D}{a^3} \gamma^3 [U_2(\xi) + a_1 U_4(\xi) + b_1 U_1(\xi)], \quad (55)$$

takes zero value at $\xi=0$, i.e. $Q(0) = -D\gamma^3 b_1 / a^3 = 0$. This condition is related to $b_1=0$ and according to Eq. (54), one obtains eigenvalue equation $th\gamma + tg\gamma = 0$, with roots Eq. (5).

In similar way, bending moment of the second shape function:

$$M(\xi) = -D \frac{d^2 X}{d\xi^2} = -\frac{D}{a^2} \gamma^2 [U_4(\xi) + a_2 U_1(\xi) + b_2 U_2(\xi)], \quad (56)$$

takes zero value at $\xi=0$, i.e. $M(0) = -D\gamma^2 a_2 / a^2 = 0$. Taking into account that $a_2=0$, Eq. (54), eigenvalue function $th\gamma - tg\gamma = 0$ is obtained with eigenvalues Eq. (6).

Finite element is constructed with beam shape functions $X_1(\xi)$ and $X_3(\xi)$ with argument $\gamma_2 = 2.3650$, and $X_2(\xi)$ and $X_4(\xi)$ with argument $\gamma_3 = 3.9266$. Similar expressions to Eq. (53) can be written for beam functions in η direction $Y_i(\eta)$, $i = 1, 2, 3, 4$ with corresponding Krylov function $V_j(\eta)$, $j = 1, 2, 3, 4$. For derivatives of Krylov functions, relations in Eq. (50) are available. Stiffness and mass matrix are specified by Eqs. (44) and (46), respectively.

The first two beam shape functions expressed by Krylov functions are shown in Figures 5 and 6 and compared with ordinary beam shape functions known as Hermite polynomials [1]. The difference between $X_i(\xi)$ values is small, whereas the one between $X_i''(\xi)$ values is larger. Polynomial $X_i''(\xi)$ function is a straight line, and that expressed by Krylov functions is of parabolic shape. Curvature functions $X_i''(\xi)$ influence the stiffness matrix and deflection functions $X_i(\xi)$ influence mass matrix. If shape function $X_2(\xi)$ is defined with γ_2 , it is very close to the polynomial shape function, Figure 6. For $\gamma \leq 0.1$, shape functions in terms of Krylov functions give the same numerical values as Hermite polynomials, Figures 5 and 6. If trigonometric and hyperbolic functions in Krylov functions Eq. (48) and coefficients Eq. (54) are expanded into power series and setting $\gamma \rightarrow 0$, shape functions Eq. (53) are reduced to polynomial beam shape functions in Eq. (4).

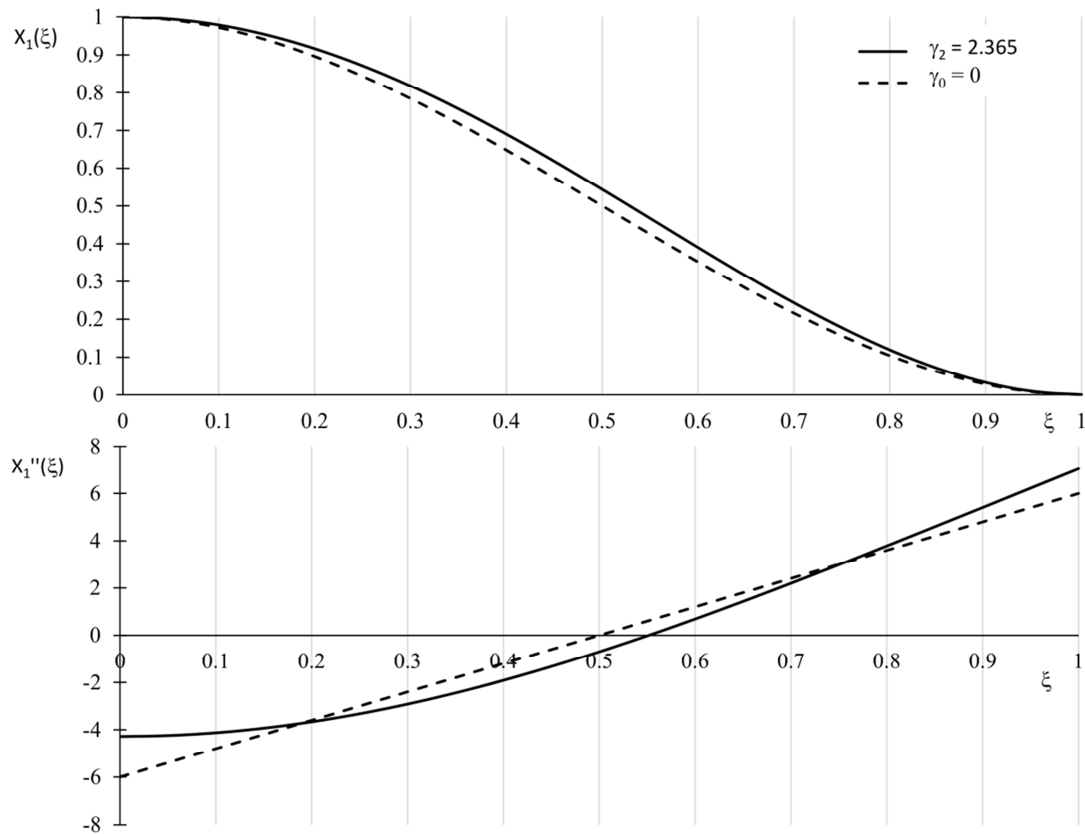


Fig. 5 Comparison of the first beam shape function determined by Krylov functions and polynomial

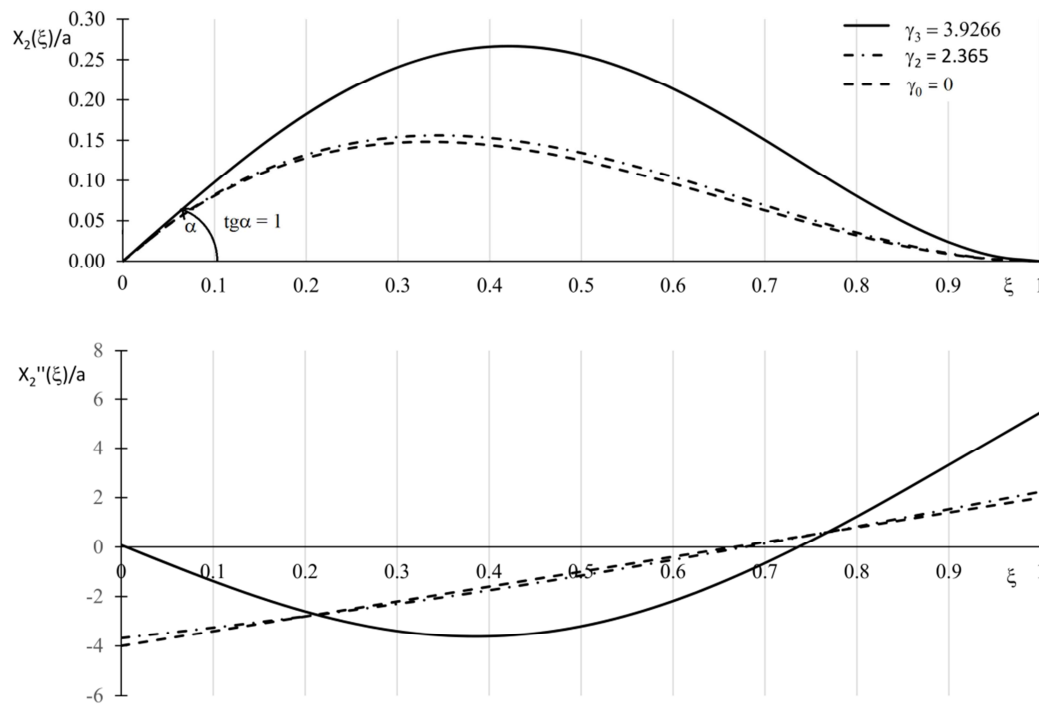


Fig. 6 Comparison of the second beam shape function determined by Krylov functions and polynomial

In order to investigate the accuracy of different finite element formulations, vibration analysis of clamped square plate is performed. Plate is modelled by different mesh density, and corresponding fractions of parameters γ_2 and γ_3 . The obtained results for the first 8 natural modes are shown in Table 3, and compared with the Liew values [13]. Mesh 2x2 with γ_2 and γ_3 gives only the first three natural frequencies due to only one central free node with 3 d.o.f., which are highly accurate. For mesh 4x4 discrepancies are increased, but values of frequency parameter converge to the accurate values, Table 3.

Table 3 Frequency parameter $\Omega = \omega(b/\pi)^2 \sqrt{\rho h/D}$ of clamped square plate, dynamic shape functions, $\gamma_2 = 2.3650$, $\gamma_3 = 3.9266$

Mesh	γ_2, γ_3	Mode 1	Mode 2	Mode 3	Mode 4	Mode 5	Mode 6	Mode 7	Mode 8
2x2	γ_2, γ_3	3.6586 (0.34%)	7.4711 (0.47%)	7.4711 (0.47%)					
4x4	$\gamma_2/2, \gamma_3/2$	3.7280	7.5951	7.5951	11.3222	13.5952	13.7220	17.1954	17.1954
6x6	$\gamma_2/3, \gamma_3/3$	3.7111	7.5713	7.5713	11.3234	13.5663	13.6225	17.2919	17.2919
8x8	$\gamma_2/4, \gamma_3/4$	3.7012	7.5487	7.5487	11.2740	13.5045	13.5604	17.2123	17.2123
10x10	$\gamma_2/5, \gamma_3/5$	3.6957	7.5349	7.5349	11.2361	13.4719	13.5311	17.1454	17.1454
20x20	$\gamma_2/10, \gamma_3/10$	3.6877	7.5135	7.5135	11.1695	13.4267	13.4907	17.0205	17.0205
30x30	$\gamma_2/15, \gamma_3/15$	3.6861	7.5093	7.5093	11.1556	13.4185	13.4832	16.9935	16.9935
40x40	$\gamma_2/20, \gamma_3/20$	3.6856	7.5079	7.5079	11.1507	13.4158	13.4807	16.9839	16.9839
Liew [13]		3.6463	7.4364	7.4364	10.9647	13.3315	13.3951	16.7177	16.7177

If $\gamma = 0.1$ is taken into account, values of frequency parameter are equal to those determined by the static finite element with polynomial shape functions, Eqs. (4), Table 4. Values of frequency parameter converge to the exact solution by increasing finite element mesh density.

Polynomial shape functions can be presented in a simpler form, if the coordinate system of the finite element is placed in the middle of the element, Figure 3. In that case one obtains:

$$\begin{aligned} X_i &= \frac{1}{4} [2 + \xi_i \xi (3 - \xi^2)], \quad i = 1, 3 \\ X_i &= \frac{1}{16} \xi_i (4 + 3 \xi_i \xi) (\xi^2 - 1) a, \quad i = 2, 4 \\ Y_i &= \frac{1}{4} [2 + \eta_i \eta (3 - \eta^2)], \quad i = 1, 3 \\ Y_i &= \frac{1}{16} \eta_i (4 + 3 \eta_i \eta) (\eta^2 - 1) b, \quad i = 2, 4, \end{aligned} \quad (57)$$

where $-1 \leq \xi \leq 1$ and $-1 \leq \eta \leq 1$.

Stiffness and mass matrix, Eqs. (44) and (46), can be generated in symbolic form. They are the same as those in Ref. [2], since polynomials Eq. (57) can be transformed into form Eq. (4) by changing the coordinate system.

Table 4 Frequency parameter $\Omega = \omega(b/\pi)^2 \sqrt{\rho h/D}$ of clamped square plate, shape functions in terms of Krylov functions ($\gamma = 0.1$) and Hermite polynomials

Mesh	Mode 1	Mode 2	Mode 3	Mode 4	Mode 5	Mode 6	Mode 7	Mode 8
2x2	3.7473	9.4421	9.4421					
4x4	3.7238	7.6130	7.6130	11.3446	13.6324	13.7543	17.2406	17.2406
6x6	3.7110	7.5744	7.5744	11.3259	13.5780	13.6344	17.3001	17.3001
8x8	3.7013	7.5496	7.5496	11.2748	13.5076	13.5636	17.2144	17.2144
10x10	3.6957	7.5353	7.5353	11.2364	13.4730	13.5322	17.1462	17.1462
20x20	3.6877	7.5135	7.5135	11.1695	13.4268	13.4907	17.0206	17.0206
30x30	3.6861	7.5093	7.5093	11.1556	13.4185	13.4832	16.9935	16.9935
40x40	3.6856	7.5079	7.5079	11.1507	13.4158	13.4807	16.9839	16.9839
Liew [13]	3.6463	7.4364	7.4364	10.9647	13.3315	13.3951	16.7177	16.7177

5. STRIP FINITE ELEMENT FOR SIMPLY SUPPORTED PLATE AT TWO OPPOSITE EDGES

5.1 THEORETICAL CONSIDERATION

Differential equation of plate vibration reads [4]:

$$\frac{\partial^4 W}{\partial x^4} + 2 \frac{\partial^4 W}{\partial x^2 \partial y^2} + \frac{\partial^4 W}{\partial y^4} - \omega^2 \frac{\bar{m}}{D} W = 0. \quad (58)$$

In case of simply supported longitudinal edges one can assume deflection in the form:

$$W(\xi, \eta) = X(\xi) \sin \gamma \eta, \quad \gamma = n\pi, \quad n = 1, 2, \dots \quad (59)$$

By substituting Eq. (59) into Eq. (58), ordinary differential equation of Lévy form is obtained [4]:

$$X'''' - 2\left(\frac{a}{b}\right)^2 \gamma^2 X'' + \left[\left(\frac{a}{b}\right)^4 \gamma^4 - \omega^2 \frac{\bar{m}a^4}{D}\right] X = 0. \quad (60)$$

Solution of Eq. (60) is assumed in the exponential form $X = e^{\lambda\xi}$ and four roots are obtained, i.e. $\lambda_{1,2} = \pm\alpha$, $\lambda_{3,4} = \pm i\beta$, where:

$$\alpha = \sqrt{\omega a^2 \sqrt{\frac{\bar{m}}{D}} + \left(\frac{a}{b}\right)^2 \gamma^2}, \quad \beta = \sqrt{\omega a^2 \sqrt{\frac{\bar{m}}{D}} - \left(\frac{a}{b}\right)^2 \gamma^2}. \quad (61)$$

Hence, deflection function Eq. (59) and rotation angle Eq. (2) read:

$$W(\xi, \eta) = X(\xi) \sin \gamma \eta, \quad \psi(\xi, \eta) = -\frac{\partial W}{\partial x} = \Psi(\xi) \sin \gamma \eta, \quad (62)$$

where:

$$\begin{aligned} X(\xi) &= A_1 \sinh \gamma \eta + A_2 \cosh \gamma \eta + A_3 \sin \beta \xi + A_4 \cos \beta \xi, \\ \Psi(\xi) &= -\frac{1}{a} (A_1 \alpha \cosh \alpha \xi + A_2 \alpha \sinh \alpha \xi + A_3 \beta \cos \beta \xi - A_4 \beta \sin \beta \xi) \sin \gamma \eta. \end{aligned} \quad (63)$$

Bending moment and total shearing force, according to Ref. [4], read:

$$\begin{aligned} M_x(\xi, \eta) &= -D \left(\frac{\partial^2 W}{\partial x^2} + \nu \frac{\partial^2 W}{\partial y^2} \right) = M_x^0(\xi) \sin \gamma \eta, \\ \bar{Q}_x(\xi, \eta) &= -D \left[\frac{\partial^3 W}{\partial x^3} + (2 - \nu) \frac{\partial^3 W}{\partial x \partial y^2} \right] = \bar{Q}_x^0(\xi) \sin \gamma \eta, \end{aligned} \quad (64)$$

where:

$$\begin{aligned} M_x^0(\xi) &= -D (A_1 c_1 \sinh \alpha \xi + A_2 c_1 \cosh \alpha \xi - A_3 c_2 \sin \beta \xi - A_4 c_2 \cos \beta \xi), \\ \bar{Q}_x^0(\xi) &= -D (A_1 d_1 \cosh \alpha \xi + A_2 d_1 \sinh \alpha \xi - A_3 d_2 \cos \beta \xi + A_4 d_2 \sin \beta \xi), \end{aligned} \quad (65)$$

and:

$$\begin{aligned} c_1 &= \left(\frac{\alpha}{a}\right)^2 - \nu \left(\frac{\gamma}{b}\right)^2, \quad c_2 = \left(\frac{\beta}{a}\right)^2 + \nu \left(\frac{\gamma}{b}\right)^2, \\ d_1 &= \left[\left(\frac{\alpha}{a}\right)^2 - (2 - \nu) \left(\frac{\gamma}{b}\right)^2 \right] \frac{\alpha}{a}, \quad d_2 = \left[\left(\frac{\beta}{a}\right)^2 + (2 - \nu) \left(\frac{\gamma}{b}\right)^2 \right] \frac{\beta}{a}. \end{aligned} \quad (66)$$

Nodal displacements $X(0) = X_1$, $\Psi(0) = \Psi_1$, $X(1) = X_2$ and $\Psi(1) = \Psi_2$ can be written in the matrix notation:

$$\begin{Bmatrix} X_1 \\ \Psi_1 \\ X_2 \\ \Psi_2 \end{Bmatrix} = \begin{bmatrix} 0 & 1 & 0 & 1 \\ -\frac{\alpha}{a} & 0 & -\frac{\beta}{a} & 0 \\ \sinh \alpha & \cosh \alpha & \sin \beta & \cos \beta \\ -\frac{\alpha}{a} \cosh \alpha & -\frac{\alpha}{a} \sinh \alpha & -\frac{\beta}{a} \cos \beta & \frac{\beta}{a} \sin \beta \end{bmatrix} \begin{Bmatrix} A_1 \\ A_2 \\ A_3 \\ A_4 \end{Bmatrix}. \quad (67)$$

On the other side nodal forces $\bar{Q}_x^0(0) = -Q_1$, $M_x^0(0) = -M_1$, $\bar{Q}_x^0(1) = Q_2$ and $M_x^0(1) = M_2$ are also presented in the matrix notation:

$$\begin{Bmatrix} Q_1 \\ M_1 \\ Q_2 \\ M_2 \end{Bmatrix} = D \begin{bmatrix} d_1 & 0 & -d_2 & 0 \\ 0 & c_1 & 0 & -c_2 \\ -d_1 \cosh \alpha & -d_1 \sinh \alpha & d_2 \cos \beta & -d_2 \sin \beta \\ -c_1 \sinh \alpha & -c_1 \cosh \alpha & c_2 \sin \beta & c_2 \cos \beta \end{bmatrix} \begin{Bmatrix} A_1 \\ A_2 \\ A_3 \\ A_4 \end{Bmatrix}. \quad (68)$$

Equations (67) and (68) can be written in a condensed matrix form $\{\delta\} = [B]\{A\}$ and $\{F\} = [C]\{A\}$, and by eliminating vector $\{A\}$, the strip finite element equation is obtained:

$$\{F\} = [K(\omega)]\{\delta\}, \quad (69)$$

where:

$$[K(\omega)] = [C][B]^{-1}, \quad (70)$$

is 4x4 symmetric dynamic stiffness matrix with 6 independent terms shown in the Appendix.

Equation (69) is derived by the displacement finite element method. In some cases, it is more convenient to use the finite element equation obtained by the force finite element approach, i.e.

$$\{\delta\} = [L(\omega)]\{F\}, \quad (71)$$

where:

$$[L(\omega)] = [K(\omega)]^{-1} = [B][C]^{-1}, \quad (72)$$

is dynamic flexibility matrix [2]. Its terms are also given in the Appendix.

A plate with uniform stiffness and mass distribution is modelled by only one or two strip elements, depending on boundary conditions. For each value of $\gamma = n\pi$, $n = 1, 2, \dots$ infinite number of exact natural frequencies and modes can be theoretically determined. If natural vibrations of a plate with variable properties in longitudinal direction is analysed, plate is modelled by a set of strip finite elements. Natural frequencies are determined from condition $\text{Det}[K_s(\omega)] = 0$.

5.2 ILLUSTRATIVE EXAMPLES

Simply supported square plate, SSSS

Only one strip finite element is sufficient to solve this task with combined geometric and physical boundary conditions. By taking into account boundary conditions $X_1 = X_2 = 0$, the finite element equation is reduced to two d.o.f. system:

$$\begin{Bmatrix} M_1 \\ M_2 \end{Bmatrix} = \begin{bmatrix} k_{22} & k_{24} \\ k_{42} & k_{44} \end{bmatrix} \begin{Bmatrix} \Psi_1 \\ \Psi_2 \end{Bmatrix}. \quad (73)$$

Since $k_{44} = k_{22}$ and $k_{42} = k_{24}$ one can write for the determinant of Eq. (73):

$$\text{Det} = (k_{22} + k_{24})(k_{22} - k_{24}) = 0. \quad (74)$$

Each of the above expressions in the brackets can be equal to zero. By applying formulae (A1) from the Appendix, the following is obtained:

$$k_{22} \pm k_{24} = \frac{a}{D_k} (c_1 + c_2) [\alpha \sin \beta (\cosh \alpha \mp 1) - \beta \sinh \alpha (1 \mp \cos \beta)] = 0. \quad (75)$$

Deflection of a simply supported plate is described only by trigonometric functions, and excluding hyperbolic functions from Eq. (75), one finds $\sin \beta = 0$, i.e. $\beta = m\pi$. Finally, by employing the second formula of Eq. (61) for β , the well-known formula for natural frequencies of simply supported plate is obtained:

$$\omega = \left[\left(\frac{m\pi}{a} \right)^2 + \left(\frac{n\pi}{b} \right)^2 \right] \sqrt{\frac{D}{m}}. \quad (76)$$

Dimensionless frequency parameter:

$$\Omega = \omega \left(\frac{b}{\pi} \right)^2 \sqrt{\frac{m}{D}}, \quad (77)$$

takes the simple form:

$$\Omega = \left(\frac{b}{a} \right)^2 m^2 + n^2. \quad (78)$$

Values of Ω for square plate are compared with those determined numerically by Rayleigh-Ritz method in Ref. [13], Table 5.

Table 5 Frequency parameter $\Omega = (\omega b^2 / \pi^2) \sqrt{\rho h / D}$ of square plate simply supported at longitudinal edges

Mode no.	SSSS			CSCS			FSFS		
	$m \times n$	Exact	Liew, [13]	n	Exact	Liew, [13]	n	Exact	Liew, [13]
1	1 x 1	2	2.0000	1	2.9354	2.9334	1	0.9781	0.9768
2	2 x 1	5	5.0000	2	5.5484	5.5465	1	1.6352	1.6355
3	1 x 2	5	5.0000	1	7.0304	7.0242	1	3.7234	3.7215
4	2 x 2	8	8.0000	2	9.5893	9.5833	2	3.9456	3.9462
5	3 x 1	10	9.9999	3	10.3580	10.3564	2	4.7362	4.7357
6	1 x 3	10	9.9999	1	13.0920	13.0797	2	7.1703	7.1674
7	3 x 2	13	12.9998	3	14.2109	14.2053	1	7.6340	7.6278
8	2 x 3	13	12.9998	2	15.6937	15.6815	3	8.9147	8.9149
9	4 x 1	17	16.9995	4	17.2604	17.2597	3	9.7314	9.7309
10	1 x 4	17	16.9995	3	20.2561	20.2442	2	11.2557	11.2489

Clamped square plate at transverse edges, CSCS

This problem with geometric boundary conditions at transverse edges can be solved with at least two strip finite elements. By taking into account boundary conditions, the reduced assembly equation reads:

$$\begin{Bmatrix} Q_2 \\ M_2 \end{Bmatrix} = \begin{bmatrix} k_{33}^{(1)} + k_{11}^{(2)} & k_{34}^{(1)} + k_{12}^{(2)} \\ k_{43}^{(1)} + k_{21}^{(2)} & k_{44}^{(1)} + k_{22}^{(2)} \end{bmatrix} \begin{Bmatrix} X_2 \\ \Psi_2 \end{Bmatrix}, \quad (79)$$

where $k_{ij}^{(p)}$, $p=1,2$ are related to strip elements, and Q_2 , M_2 , X_2 and Ψ_2 are related to the middle node of the assembly. Since two finite elements are equal, one can write according to Eqs. (A1):

$$k_{33}^{(1)} = k_{11}^{(2)} = k_{11}, k_{44}^{(1)} = k_{22}^{(2)} = k_{22}, k_{34}^{(1)} = -k_{12}^{(2)}. \quad (80)$$

Determinant of Eq. (79) reads:

$$\begin{aligned} Det = 4k_{11}k_{22} &= \frac{4a}{D_K^2} (d_2\alpha + d_1\beta)(c_1 + c_2) \cdot \\ &(\alpha sh\alpha \cos\beta + \beta ch\alpha \sin\beta)(\alpha ch\alpha \sin\beta - \beta sh\alpha \cos\beta) = 0. \end{aligned} \quad (81)$$

Two transcendental frequency equations are obtained from Eq. (81), i.e.

$$\alpha th\alpha + \beta tg\beta = 0, \beta th\alpha - \alpha tg\beta = 0. \quad (82)$$

The former and the latter are related to symmetric and antisymmetric modes, respectively. Taking into account Eqs. (61), values of frequency parameter Ω , Eq. (77), are determined for square plate and listed in Table 5. That exact solutions are compared with numerical values calculated by the Rayleigh-Ritz method in Ref. [13].

Free square plate at transverse edges, FSFS

Due to physical boundary conditions at the transverse edges, it is more convenient to solve this task by using the forced finite element formulation and at least two strip elements. Taking boundary conditions into account, the reduced assembly equation takes the form:

$$\begin{Bmatrix} X_2 \\ \Psi_2 \end{Bmatrix} = \begin{bmatrix} l_{33}^{(1)} + l_{11}^{(2)} & l_{34}^{(1)} + l_{12}^{(2)} \\ l_{43}^{(1)} + l_{21}^{(2)} & l_{44}^{(1)} + l_{22}^{(2)} \end{bmatrix} \begin{Bmatrix} Q_2 \\ M_2 \end{Bmatrix}, \quad (83)$$

where $l_{ij}^{(p)}$, $p=1,2$ are elements of the dynamic flexibility matrix Eq. (79) for two elements. In similarity to the previous example, according to Eqs. (A2):

$$l_{33}^{(1)} = l_{11}^{(2)} = l_{11}, l_{44}^{(1)} = l_{22}^{(2)} = l_{22}, l_{34}^{(1)} = -l_{12}^{(2)}. \quad (84)$$

and the determinant of Eq. (84) reads:

$$\begin{aligned} Det = 4l_{11}l_{22} &= \frac{4}{D_L^2 a} (d_2\alpha + d_1\beta)(c_1 + c_2) \cdot \\ &\cdot (c_2 d_1 ch\alpha \sin\beta - c_1 d_2 sh\alpha \cos\beta)(c_1 d_2 ch\alpha \sin\beta + c_2 d_1 sh\alpha \cos\beta) = 0. \end{aligned} \quad (85)$$

Two transcendental frequency equations are obtained from Eq. (85), i.e.

$$c_1 d_2 th\alpha - c_2 d_1 tg\beta = 0, c_2 d_1 th\alpha + c_1 d_2 tg\beta = 0. \quad (86)$$

The former and latter are related to antisymmetric and symmetric modes, respectively. By employing relations (61), values of the frequency parameter Ω , Eq. (77), are determined for the square plate and included in Table 5. They are compared with numerically determined values from Ref. [13].

In the literature, the above task is solved by employing ordinary used displacement finite element method and only one finite element. However, in that case one is faced with the problem of natural frequencies determination since $Det[K(\omega)] \neq 0$. This problem is overcome

by a special and rather complex Wittrick-Williams algorithm [5, 6]. However, by using the force finite element formulation for similar problems, the solution is obtained straight away and unnecessary complications are avoided.

6. CONCLUSION

Nowadays, dynamic finite elements with frequency dependent properties are more and more used, due to course finite element mesh and high accuracy. If analytical solution of the considered issue is applied, a unique dynamic stiffness matrix is constructed and exact results are obtained. If free beam natural modes are used for describing plate deflection, the energy approach is employed and static stiffness and mass matrix are derived.

The latter approach is used for the construction of a non-conforming 4-noded rectangular plate finite element (Section 3). Course mesh gives approximate results for the spectrum of natural frequencies quite close to the exact ones. In case of a conforming finite element with shape functions as product of dynamic beam shape functions, only the first few natural frequencies are close to the exact values (Section 4). By increasing finite element mesh density and decreasing values of argument of trigonometric and hyperbolic functions accordingly, the obtained results converge to the exact ones. If a very small value of that argument is used, dynamic shape functions become equal to static shape functions, and static finite element is obtained with ordinary convergence of numerical results.

In case of plate simply supported at two opposite edges, 2D problem is reduced to 1D, i.e. strip element, with closed-form analytical solution. Dynamic stiffness matrix based on that solution gives exact values of natural frequencies for any combination of boundary condition at the remaining two plate edges.

The developed 4-noded dynamic finite elements are not reliable for a wider practical use. On the contrary, application of the 2-noded strip dynamic finite element is very effective. In future research, the same approach can be used for the development of a 2-noded finite element for thick plates, by employing the modified Mindlin theory [14].

7. ACKNOWLEDGEMENT

This work was supported by the National Research Foundation of Korea (NRF) grant funded by the Korean Government (MSIP) through GCRC-SOP (Grant No. 2011-0030669).

8. APPENDIX: DYNAMIC STIFFNESS AND FLEXIBILITY MATRIX OF THE PLATE SIMPLY SUPPORTED AT TWO OPPOSITE EDGES

Elements of dynamic stiffness matrix according to Eqs. (67), (68) and (70):

$$\begin{aligned}
 k_{11} &= k_{33} = \frac{1}{D_K} (d_2 \alpha + d_1 \beta) (\alpha \operatorname{sh} \alpha \cos \beta + \beta \operatorname{ch} \alpha \sin \beta), \\
 k_{12} &= -k_{34} = -\frac{a}{D_K} [(d_2 \alpha - d_1 \beta) (\operatorname{ch} \alpha \cos \beta - 1) + (d_1 \alpha + d_2 \beta) \operatorname{sh} \alpha \sin \beta], \\
 k_{13} &= -\frac{1}{D_K} (d_2 \alpha + d_1 \beta) (\alpha \operatorname{sh} \alpha + \beta \sin \beta), \\
 k_{14} &= -k_{23} = -\frac{a}{D_K} (d_2 \alpha + d_1 \beta) (\operatorname{ch} \alpha - \cos \beta), \\
 k_{22} &= k_{44} = \frac{a}{D_K} (c_1 + c_2) (\alpha \operatorname{ch} \alpha \sin \beta - \beta \operatorname{sh} \alpha \cos \beta), \\
 k_{24} &= \frac{a}{D_K} = (c_1 + c_2) (\beta \operatorname{sh} \alpha - \alpha \sin \beta), \\
 D_K &= 2\alpha\beta(1 - \operatorname{ch} \alpha \cos \beta) + (\alpha^2 - \beta^2) \operatorname{sh} \alpha \sin \beta.
 \end{aligned} \tag{A1}$$

Elements of dynamic flexibility matrix according to Eqs. (67), (68) and (72):

$$\begin{aligned}
 l_{11} &= l_{33} = -\frac{1}{D_L} (c_1 + c_2) (c_2 d_1 \operatorname{ch} \alpha \sin \beta - c_1 d_2 \operatorname{sh} \alpha \cos \beta), \\
 l_{12} &= -l_{34} = -\frac{1}{D_L} [d_1 d_2 (c_1 - c_2) (1 - \operatorname{ch} \alpha \cos \beta) + (c_1 d_2^2 + c_2 d_1^2) \operatorname{sh} \alpha \sin \beta], \\
 l_{13} &= \frac{1}{D_L} (c_1 + c_2) (c_1 d_2 \operatorname{sh} \alpha - c_2 d_1 \sin \beta), \\
 l_{14} &= -l_{23} = -\frac{1}{D_L} d_1 d_2 (c_1 + c_2) (\operatorname{ch} \alpha - \cos \beta), \\
 l_{22} &= l_{44} = -\frac{1}{D_L a} (d_2 \alpha + d_1 \beta) (c_1 d_2 \operatorname{ch} \alpha \sin \beta + c_2 d_1 \operatorname{sh} \alpha \cos \beta), \\
 l_{24} &= -\frac{1}{D_L a} = (d_2 \alpha + d_1 \beta) (c_2 d_1 \operatorname{sh} \alpha + c_1 d_2 \sin \beta), \\
 D_L &= 2c_1 c_2 d_1 d_2 (1 - \operatorname{ch} \alpha \cos \beta) + (c_2^2 d_1^2 - c_1^2 d_2^2) \operatorname{sh} \alpha \sin \beta.
 \end{aligned} \tag{A2}$$

9. REFERENCES

- [1] O.C. Zienkiewicz, *The Finite Element Method in Engineering Science*, McGraw-Hill, New York, 1971.
- [2] J.S. Przemieniecki, *Theory of Matrix Structural Analysis*, McGraw-Hill, New York, 1968.
- [3] D.J. Dawe, *Matrix and Finite Elements Displacement Analysis of Structures*, Clarendon Press, Oxford, 1984.
- [4] R. Szilard, *Theory and Applications of Plate Analysis*, John Wiley & Sons, Hoboken, 2004.

- [5] M. Boscolo, J.R. Banerjee, Dynamic stiffness formulation for plates using first order shear deformation theory, 51st AIAA/ASME/ASCE/AHS/ASC Structures, *Structural Dynamics, and Materials Conference*
 18th 12-15 April 2010, Orlando, Florida.
- [6] F.W. Williams, S. Yuan, K. Ye, D. Kennedy, M.S. Djoudi, Towards deep and simple understanding of transcendental eigenproblem of structural vibrations, *Journal of Sound and Vibration*, Vol. 256, No. 4, pp. 681-693, 2002.
- [7] J. Sorić, *The Finite Element Method*, Golden marketing – Tehnička knjiga, Zagreb, 2003. (in Croatian).
- [8] I. Holand, K. Bell, *Finite Element Method in Stress Analysis*, Tapir-Trykk, 1970.
- [9] I. Senjanović, *The Finite Element Method in Ship Structure Analysis*, University of Zagreb, Zagreb, 1998. (In Croatian).
- [10] Y. Xing, B. Liu, Closed form solutions for free vibrations of rectangular Mindlin plates, *Acta Mechanica Sinica*, Vol. 25, No. 5, pp. 689-698, 2009.
- [11] I. Senjanović, M. Tomić, N. Vladimir, D.S. Cho, Analytical solution for free vibration of a moderately thick rectangular plate, Hindawi Publishing Corporation, *Mathematical Problems in Engineering*, Volume 2013, Article ID 207460.
- [12] I. Senjanović, M. Tomić, N. Vladimir, An approximate analytical procedure for natural vibration analysis of free rectangular plates, *Thin-Walled Structures*, Vol. 95, pp. 101-114, 2015.
- [13] K.M. Liew, Y. Xiang, S. Kitipornchai, Transverse Vibration of Thick Rectangular Plates – I. Comprehensive Set of Boundary Conditions, *Computers & Structures*, Vol. 49, No. 1, pp. 1-29, 1993.
- [14] I. Senjanović, N. Vladimir, M. Tomić, An advanced theory of moderately thick plate vibrations, *Journal of Sound and Vibrations*, Vol. 332, pp. 1868-1880, 2013.